I&EC research
Industrial & Engineering Chemistry Research

Article

Cite This: Ind. Eng. Chem. Res. 2019, 58, 19211−19225

pubs.acs.org/IECR

Novel Process Design Combined with Reactive Distillation and Pressure-Swing Distillation for Propylene Glycol Monomethyl Ether Acetate Synthesis

Yufeng Fan, Qing Ye,* Hao Cen, Jingxing Chen, and Tong Liu

Jiangsu Key Laboratory of Advanced Catalytic Materials and Technology, School of Petrochemical Engineering, Changzhou University, Changzhou, Jiangsu 213164, China

ABSTRACT: A reactive distillation and pressure-swing distillation combined process (RDPSD) for propylene glycol monomethyl ether acetate synthesis is proposed in this study. The energy requirements of RDPSD can be reduced by the introduction of heat integration. Furthermore, the vapor recompression is used in the RDPSD to enhance the energy-saving performance. Finally, the RDPSD with vapor recompression (RDPSDVR) is optimized through the heat exchanger network (HEN) for further reduction of energy consumption. The proposed processes are compared in total annual cost (TAC), total energy requirements (TER), and CO_2 emissions. Based on the result of comparison of proposed processes, the RDPSDVR combined with HEN (RDPSDVR-R-L-HEN) shows the best performance. The RDPSDVR-R-L-HEN decreases by 51.83% of the TAC, 57.87% of the TER, and 62.15% of the CO_2 emissions compared with that of the two-column RD, respectively.

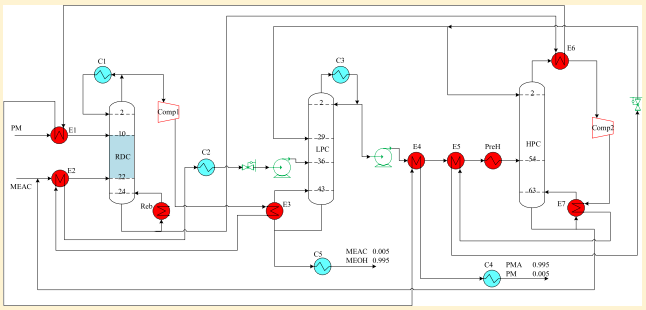

1. INTRODUCTION

Propylene glycol monomethyl ether acetate (PMA) has been used as an active solvent for multiple industrial applications. The esterification reaction between propylene glycol monomethyl ether (PM) and acetic acid catalyzed by the acid catalyst is a common route for the PMA production.[1] It should be mentioned that the acid catalyst may make the generation of the acidic PMA, which does not meet the demand of the industrial grade PMA. Wang et al.[2] proposed a synthesis method for PMA via a transesterification reaction between PM and methyl acetate (MEAC). This reaction is catalyzed through the basic homogeneous catalyst sodium methoxide so that the acidic PMA can be avoided.

In order to solve the problem of thermodynamic limitations in reactions like transesterification reaction and esterification, the reactive distillation (RD) is a good choice which can improve the reaction conversion.[3] Qiu et al.[4] proposed an RD process for isopropyl alcohol synthesis through the transesterification reaction of isopropyl acetate with methanol, which has high conversion compared with the direct hydration process. Jiménez et al.[5] explored a butyl acetate synthesis process where the RD process is added to overcome the unfavorable chemical equilibrium. In recent studies about transesterification reactions, many RD processes have been developed. Suo et al.[6] designed a novel RD process for the manufacturing of isobutyl acetate via the transesterification reaction between methyl acetate and isobutanol. Shen et al.[7] explored the RD process for the transesterification reaction of methyl acetate and n-propanol. Fan et al.[8] designed the RD process for isopropyl alcohol production via the transesterification reaction of isopropyl acetate with methanol. In these RD processes for the transesterification reaction, there are two columns; one is the RD column (RDC) where the transesterification reaction occurs, and the other is the conventional distillation column for the separation of the azeotrope. In order to make the transesterification reaction in the RDC proceed, the azeotrope is recycled back to RDC with a high flow rate. Thus, a quantity of energy is required in the RD process. One issue should be noted that the MEOH-MEAC azeotrope is generated in the PMA synthesis process. Therefore, to save energy consumption in the RD process for the PMA synthesis, the pure material recycle stream of the RD process which can be achieved by separating the azeotropes is considered.

For the separation of the azeotropes, the pressure-swing distillation (PSD) can be a wise choice. The PSD is an effective method to separate the azeotrope when the azeotropic composition changes significantly with the operating pressure of column changes.[9] Cui et al.[10] explored a PSD process to separate the water/benzene/isopropyl alcohol system and compared the PSD configuration and the heterogeneous azeotropic distillation configuration. Yang et al.[11] developed a triple-column PSD process to separate ternary systems with three binary minimum azeotropes, and the operating conditions

Received: July 27, 2019
Revised: September 12, 2019
Accepted: September 23, 2019
Published: September 23, 2019

DOI: 10.1021/acs.iecr.9b04122
Ind. Eng. Chem. Res. 2019, 58, 19211−19225

of the PSD are well controlled. Since the operating pressures of two columns of the PSD are different, there is a large temperature difference between these columns. Thus, the heat integration is used for the reduction of energy requirements of the PSD process. Abu-Elehah et al.[12] developed a heat-integrated PSD process, where the duty of reboiler in the column operated at low pressure is reduced from 1321700 to 603700 cal/h. Zhang et al.[13] designed the heat-integrated PSD process to separate the acetonitrile/methanol/benzene system. 20.09% of TAC and 35.19% of energy requirements can be saved in the partially heat-integrated processes. Luo et al.[14] improved Muñoz's PSD process by the introduction of the heat integration. Compared with the normal process, 21% of the total duty of reboiler is saved in the heat-integrated process.

Though energy requirements of the PSD process are reduced by the introduction of the heat integration, a great deal of heat is provided to the reboiler in HPC. Meanwhile, amounts of heat which is contained in the condenser of LPC is wasted. The vapor recompression technology which is one of the heat pump technology is an effective way for reduction of energy consumption of the process. In the vapor recompression process, the vapor coming from top of column is compressed and then exchanges heat with the reboiler of the process. Haelssig et al.[15] introduced a vapor recompression system into the distillation process and found that the process with vapor recompression shows the best economic performance. Ferre et al.[16] explored a vapor recompression assisted process. After combined with the vapor recompression, the economic performance of the distillation process can be further improved. Jana et al.[17] applied the vapor recompression system into the RD process. The energy requirements of the RD process with vapor recompression are 4.6% less than that of the base process. As a result, the introduction of vapor recompression technology is a good choice for further reduction of energy consumption of the PSD process. Xia et al.[18] explored a vapor recompression assisted PSD process (SHR-PSD) to separate the isopropyl alcohol/diisopropyl ether azeotrope system. 47.08% of TAC with an 8-year payback period can be saved in the SHR-PSD compared with that of the conventional PSD. Zhang et al.[19] improved the conventional PSD process by applying vapor recompression. The results indicated that the energy requirements in the PSD process could be further reduced with addition of the vapor recompression system. Li et al.[20] applied vapor recompression technology into the PSD process, and the results show that the PSD process assisted by vapor recompression achieves 62.8% of energy savings.

The heat exchanger network (HEN) according to pinch technology has been proposed by Linnhoff and Hindmarsh.[21] After combined with the HEN based on pinch technology, the hot stream of process can be utilized to generate a higher-grade utility while the cold stream of the process can be heated by a lower grade utility. Thus, the energy consumption of the process is able to be further saved by using the HEN. Yang et al.[22] used HEN to optimize the heat pump assisted process. The result indicated that the hot utility was recovered eventually, while the cold utility decreased from 188 kW to 119.2 kW. Chen et al.[23] optimized the heterogeneous azeotropic distillation process through HEN. After introduced into the HEN, the energy requirements of the previous process are reduced from 2074.0 kW to 1145.1 kW. Patraşcu et al.[24] designed a HEN on the basis of pinch analysis for the azeotropic dividing-wall column. 58% of energy requirements were decreased in the improved process compared with basic design. There are a number of studies have developed the distillation processes combined with the vapor recompression and HEN, however, few studies have introduced the vapor recompression and the HEN into the RD and PSD combined process.

This study is aimed to combine the RD process with the PSD process for the reduction of energy requirements in the base RD process; therefore, a RD and PSD combined process (RDPSD) is proposed. After the MEOH-MEAC minimum boiling azeotrope is separated through the PSD process, high mole purity MEAC with a low flow rate is flowed back into the RD part. Thus, the energy requirements of the RDPSD can be less than that of the base two-column RD process. Though the capital investment of RDPSD may increase due to the addition of the column, the RDPSD is an alternative to the conventional RD process. After comparing the two-column RD and the RDPSD in economic performance, the vapor recompression which is one of the self-heat recuperation technology and the HEN based on the pinch analysis are utilized in the better process for further improvement of the energy-saving and economic performance.

2. THERMODYNAMIC AND KINETICS MODELS

The PMA can be produced via the transesterification reaction of MEAC with PM. The PMA synthesis route is given as follows:

$$\underset{\text{MEAC}}{\text{methyl acetate}} + \underset{\text{PM}}{\text{propylene glycol methyl ether}} \leftrightarrow \underset{\text{PMA}}{\text{propylene glycol methyl ether acetate}} + \underset{\text{MEOH}}{\text{methanol}}$$

According to the Wang's[2] feasibility study on PMA synthesis by transesterification between MEAC and PM using the basic sodium methoxide as catalyst, the chemical equilibrium constant (K_{eq}) for the reaction is given as follows:

$$K_{eq} = \exp(-4963.3/T + 12.65)$$

The forward reaction rate constant (k_f) is calculated by the following equation

$$k_f = 2.96 \times 10^9 \exp(-55704/RT)$$

where T denotes kelvin absolute temperature.

On the basis of the K_{eq} and k_f, the pre-exponential factor (k_0) and activation energy (E) which are input into Aspen Plus are listed in Table 1.

Table 1. Kinetic Parameters of Transesterification Reaction of MEAC with PM

	pre-exponential factor k_0 (kmol s^{-1} m^{-3})	activation energy E (kJ mol^{-1})
positive reaction	1.14×10^{12}	55.70
negative reaction	3.66×10^{6}	14.44

Aspen Plus V8.4 is utilized for the process simulation. The MEAC-PM-PMA-MEOH quaternary system can form the MEAC-MEOH azeotrope. The vapor−liquid phase activity coefficients of the process are predicted by the nonrandom two liquid (NRTL) method. The NRTL model parameters of MEAC-MEOH, PM-PMA, MEAC-PM, MEOH-PMA, MEAC-PMA, and MEOH-PM are listed in Table 2.[2,25]

DOI: 10.1021/acs.iecr.9b04122
Ind. Eng. Chem. Res. 2019, 58, 19211−19225

Table 2. Parameters of the NRTL Method

parameter	comments					
component i	MEAC	PM	MEAC	MEOH	MEAC	MEOH
component j	MEOH	PMA	PM	PMA	PMA	PM
bij	234.866	−0.4691	541.232	422.492	604.547	114.097
bji	130.505	150.37	−276.317	−134.099	−399.086	72.0953

3. DEVELOPED PROCESSES

3.1. A Base Reactive Distillation Process. A base RD process is designed for production of PMA in this study, which is called two-column RD.

3.1.1. Economic Evaluation. In order to evaluate the economic performance of the proposed processes, the total annual cost (TAC) is selected as the method of the evaluation. The TAC is defined as the summation of the annual operating costs (OC) and the capital investments (CI) divided by a payback period (PP), which is shown as follows:

$$\mathrm{TAC} = \mathrm{OC} + \mathrm{CI}/\mathrm{PP} \quad (1)$$

An 8-year PP is used in the study. The OC contains the costs of low pressure steam (13.28 $/GJ), cooling water (0.354$/GJ), and electricity (16.8$/GJ).[26] The CI includes the costs of the column vessel, heat exchangers (condenser and reboiler), and the compressor. The basis of the economics and the sizing relationships and parameters are presented in Table 3.[27−29]

The two-column RD is optimized based on TAC. In the optimization of the two-column process, the two columns are operated at 1 atm with the stage pressure drop of 0.0027 atm. There are 14 decision design variables. Relatively, the most important among these variables that affect the total cost is the number of the rectifying stages (Nr) in the reactive distillation column (RDC), the number of the reactive stages (Nrec) in the RDC, the number of the stripping stages (Ns) in the RDC, the number of stages (NT_{SC}) in the second column (SC), and the feed location of SC (F_{SC}). These variables are optimized. There are nine key variables, the feed location of PM and MEAC are specified at the top and bottom of the reactive section respectively, the feed flow rate of PM and MEAC are specified at 50 kmol/h, the recycle flow rate is fixed at 60 kmol/h, the product PMA and MEOH purity specifications are 0.995 mole fraction, the bottom product flow rates are specified at 50 kmol/h, and the parameters of two reflux ratios (RR1 and RR2) are adjusted to meet the purity requirements of bottom products. TAC is used as the objective function, and the sequential iterative procedure is proposed for the design of the two-column RD, which is illustrated in Figure 1. The optimization steps are the following: (1) Place the reactive zone in the midsection of the reactive distillation column and pick a number for the Nrec. (2) Guess the Nr and the Ns in the reactive distillation column, respectively. (3) Vary the RR1 until the product PMA specifications are met. (4) Return to step 2 and change Nr and Ns until the TAC is minimized. (5) Return to step 1 and vary Nrec until the TAC is minimized. (6) Pick a number for the NT_{SC}. (7) Guess the F_{SC}. (8) Vary the RR2 until the product MEOH specifications are met. (9) Return to step 6 and modify NT_{RC} and F_{RC} until the TAC is minimized. Figure 2 shows the optimized flowsheet of the two-column RD. The first column is RDC where the transesterification reaction can be carried out. The total stage of the RDC is 37, and the RDC contains the rectifying section with 17 stages, the reactive section with 12 stages, and the stripping section with 8 stages. The SC is a conventional distillation column for the separation of the MEAC/MEOH mixture. The NT_{SC} is 38. The RDC and SC are operated at 1 atm. The pressure drop of each column is assumed to be 0.0027 atm. In the RDC, fresh feed of RDC is PM and MEAC with a flow rate of 50 kmol/h, which are introduced on stages 18 and 29, respectively. The MEAC/MEOH mixture with a composition of 36% mole purity MEAC and 64% mole purity MEOH is obtained from the RDC distillate and then is fed on stage 30 of SC. 50 kmol/h of 99.5% mole purity PMA is taken from the RDC bottom. The SC distillate which is the MEAC/MEOH azeotropic mixture flows back to the MEAC feed location. As shown in Figure 3, as the recycle flow rate decreases, the mole fraction of product PMA obtained from the bottom of RDC is decreased. To satisfy the required product purity, the recycle flow rate is fixed at 60 kmol/h. 99.5% mole purity MEOH is achieved from the SC bottom with a flow rate of 50

Table 3. Basis of Economics and Equipment Sizing

parameter
Heat exchangers costs
heat-transfer coefficient = 0.57 kW/K·m^2
capital cost = 7296A$^{0.65}$, where area is in squared meters
$A = \frac{Q}{U\Delta T}$, where Q is heat duty of the heat exchanger (kW) and U is the heat-transfer coefficient
Bottom heat exchangers costs
when the hot side is gas phase, heat-transfer coefficient = 0.2 kW/K·m^2
when the gas reaches its dewpoint temperature, heat-transfer coefficient = 1.2 kW/K·m^2
capital cost = 7296$A^{0.65}$, where area is in squared meters
$A = \frac{Q}{U\Delta T}$, where Q is heat duty of the heat exchanger (kW) and U is the heat-transfer coefficient
Condensers costs
heat-transfer coefficient = 0.852 kW/K·m^2
capital cost = 7296$A_c^{0.65}$, where area is in squared meters
$A_c = \frac{Q_c}{U\Delta T}$, where Q_c is heat duty of the condenser (kW) and U is the heat-transfer coefficient
Reboilers costs
heat-transfer coefficient = 0.568 kW/K·m^2
capital cost = 7296$A_R^{0.65}$, where area is in squared meters
$A_R = \frac{Q_R}{U\Delta T}$, where Q_R is heat duty of the reboiler (kW) and U is the heat-transfer coefficient
Column vessel costs
capital cost = 17640$D^{1.066}L^{0.802}$
where D is using Aspen tray sizing while L = (NT−1) × 0.61 × 1.2
Compressor costs
capital cost = 1293/280 × 1264.75 × (hp)$^{0.82}$
where hp represents the horse power of compressor (kW)
Annual steam costs
steam cost = $C_s \times Q_R \times 8000 \times 3600$
where C_s = $13.28 per GJ/LP steam (433 K)
Annual cooling water costs
cooling water cost = $0.354 \times Q_C \times 8000 \times 3600$
where Q_c is heat duty of the condenser (kW)
Electricity costs
electricity cost = 16.8 × (hp/0.6) × 8000 × 3.6/1000

DOI: 10.1021/acs.iecr.9b04122
Ind. Eng. Chem. Res. 2019, 58, 19211−19225

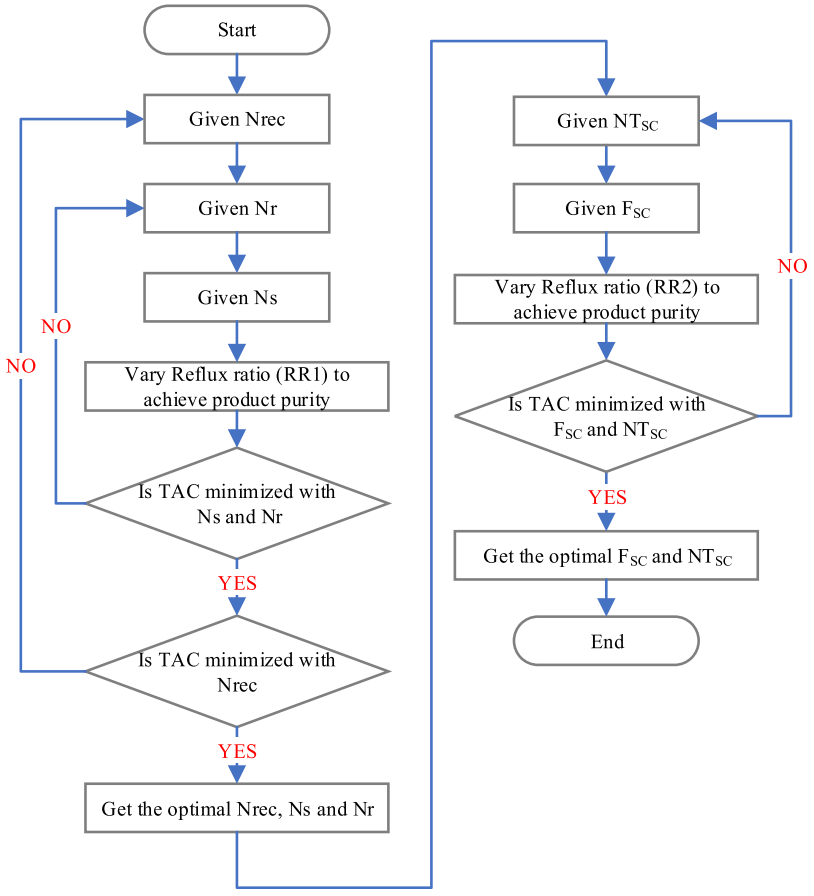

Figure 1. Sequential iterative optimization procedure for two-column RD.

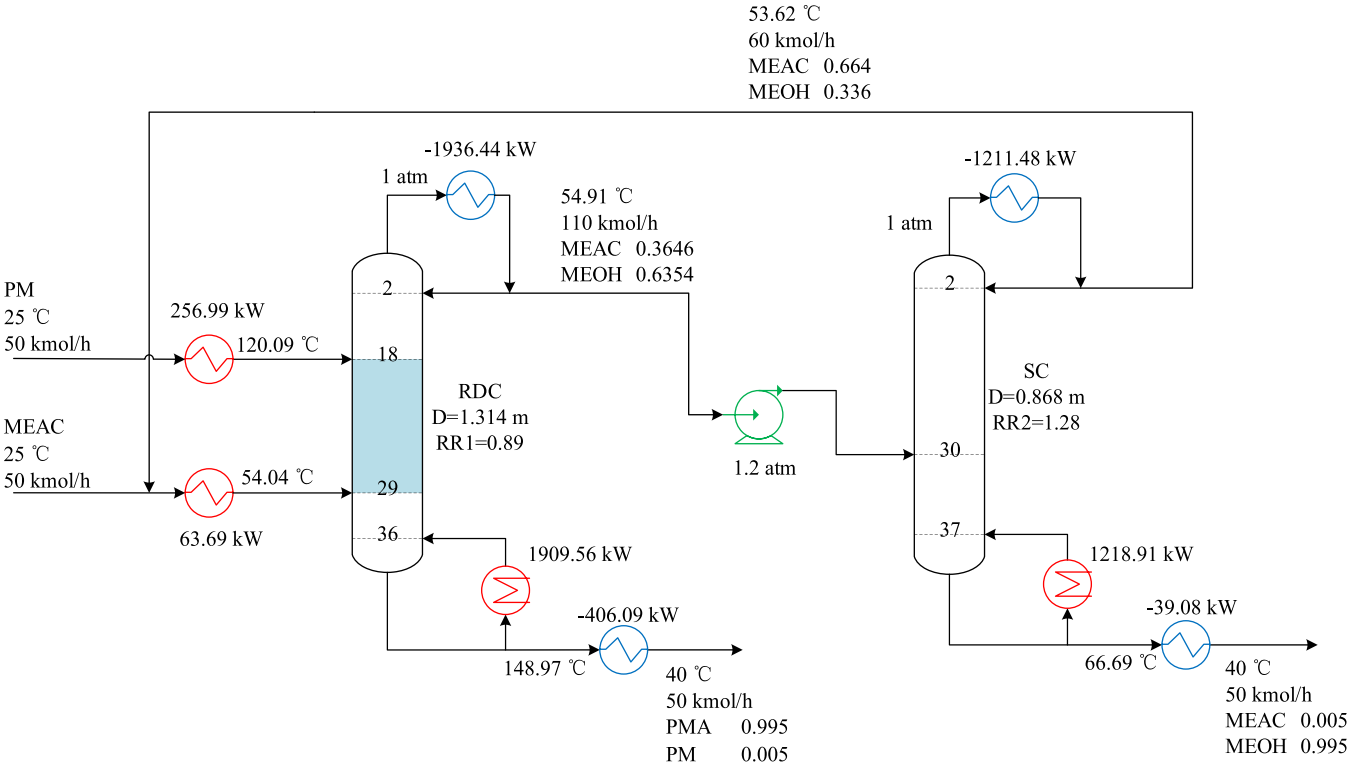

Figure 2. Flow sheet of the two-column RD.

DOI: 10.1021/acs.iecr.9b04122
Ind. Eng. Chem. Res. 2019, 58, 19211−19225

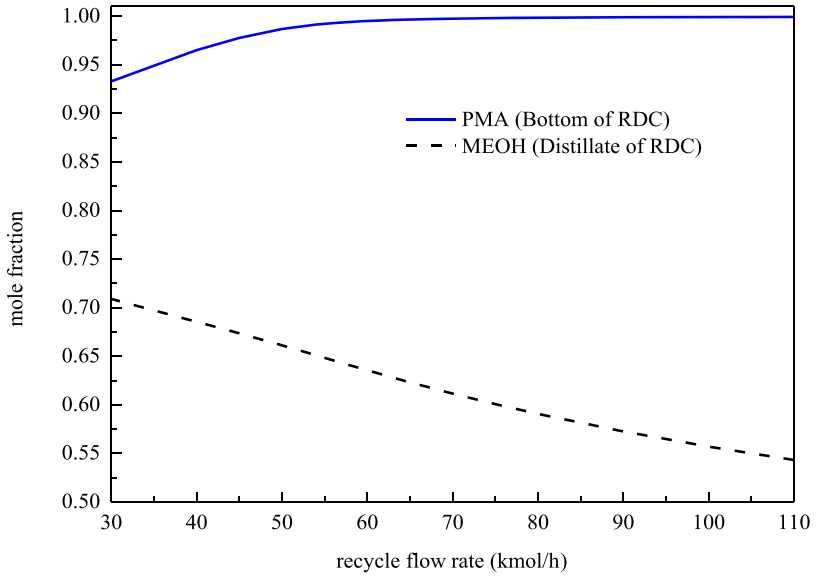

Figure 3. Effects of recycle flow rate on the mole fraction of PMA.

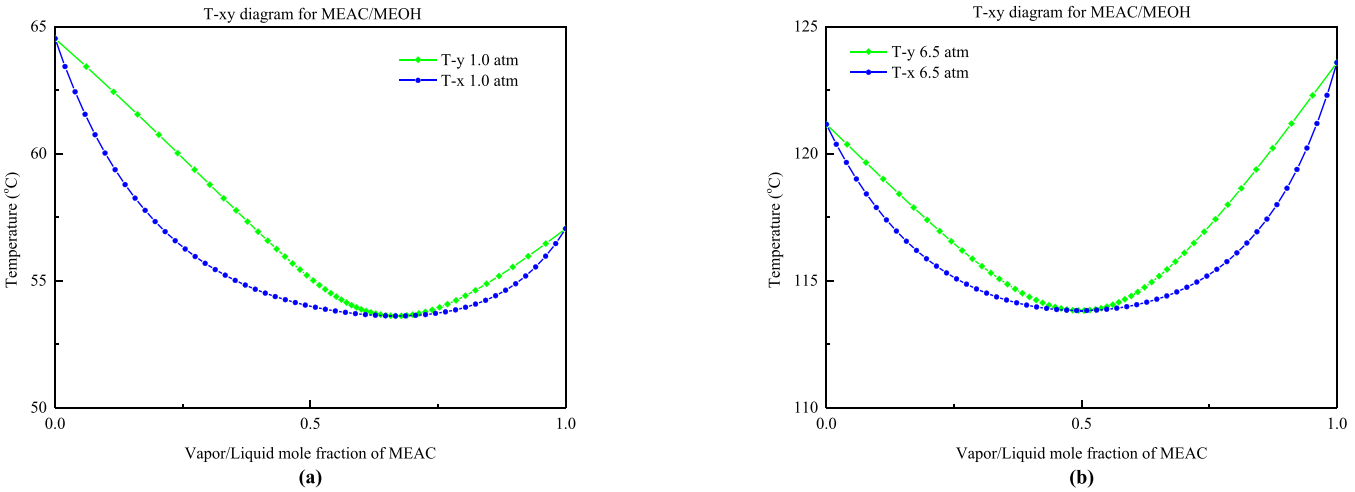

Figure 4. T-xy diagram for the MEAC/MEOH system at 1.0 atm (a) and 6.5 atm (b).

kmol/h. The TAC calculated for the two-column RD is 15.10×10^5 $.

3.2. A Reactive Distillation and Pressure-Swing Distillation Combined Process. Due to the recycle stream in the two-column RD being the MEAC-MEOH minimum boiling azeotrope, the flow rate of recycle stream should be high enough to make the transesterification reaction in the RDC proceed. Therefore, the energy requirements of the two-column RD are high. For the reduction of energy requirements in the two-column RD process, the MEOH-MEAC azeotrope can be separated before being fed back into the RDC. Thus, the PSD can be considered. The PSD process is a simple and economic technique to separate the binary homogeneous azeotrope. The separation efficiency can be enhanced with the two columns operated at different pressures. Another important inherent feature of PSD is that the energy requirements of the PSD are able to be further decreased via the introduction of heat integration. In the PSD, the temperatures across the two columns which are operated at different pressures have a great difference. Thus, the condenser of column which is operated at high pressure (HPC) is able to provide the partial or full heat to the reboiler in the column which is operated at low pressure (LPC).

The MEAC/MEOH azeotrope is sensitive to pressure. The PSD is effective in separating the azeotrope when the composition of azeotrope changes at least 5% (10% or more is better) over a proper pressure change. Figure 4 indicates that the composition of azeotrope varies from 66.7% mole purity MEAC at 1 atm to 49.8% mole purity MEAC at 6.5 atm. Thus, it is reasonable to select 1 atm for the LPC and 6.5 atm for the HPC.

As a result, the RD and PSD combined process is designed for PMA synthesis in this study, which is called RDPSD. The RDPSD is optimized based on TAC which is the same with two-column RD. Figure 5 shows the optimized flowsheet of the RDPSD. The RDPSD has three columns which are the RD column (RDC), the LPC, and the HPC, respectively. The first column is the RDC. The total stage of the RDC is 25, and the RDC contains the rectifying section (Nr) with 9 stages, the reactive section (Nrec) with 13 stages, and the stripping section (Ns) with 3 stages. The RDC is operated at 1 atm, and the pressure drop is set at 0.0027 atm. The fresh feed PM and MEAC with the flow rates of 50 kmol/h is fed on stages 10 and

DOI: 10.1021/acs.iecr.9b04122
Ind. Eng. Chem. Res. 2019, 58, 19211−19225

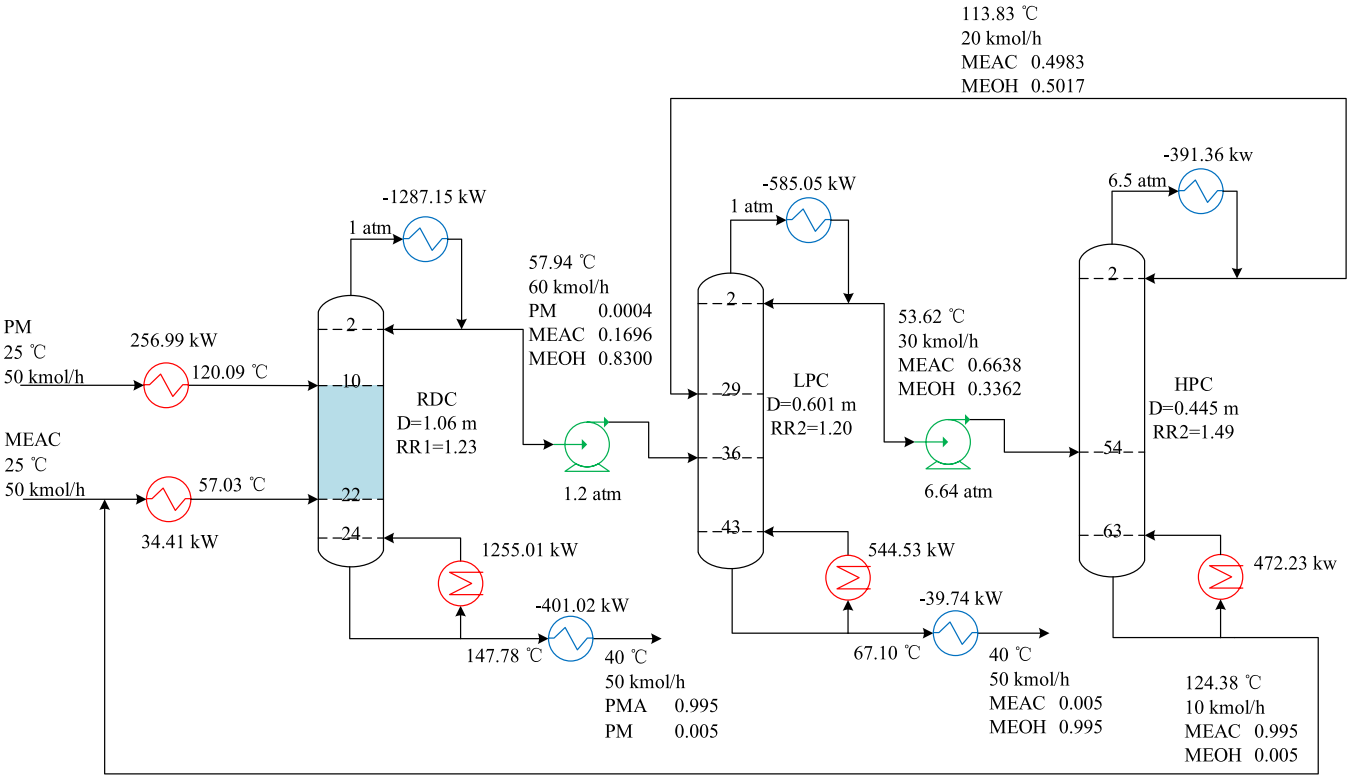

Figure 5. Flow sheet of the RDPSD.

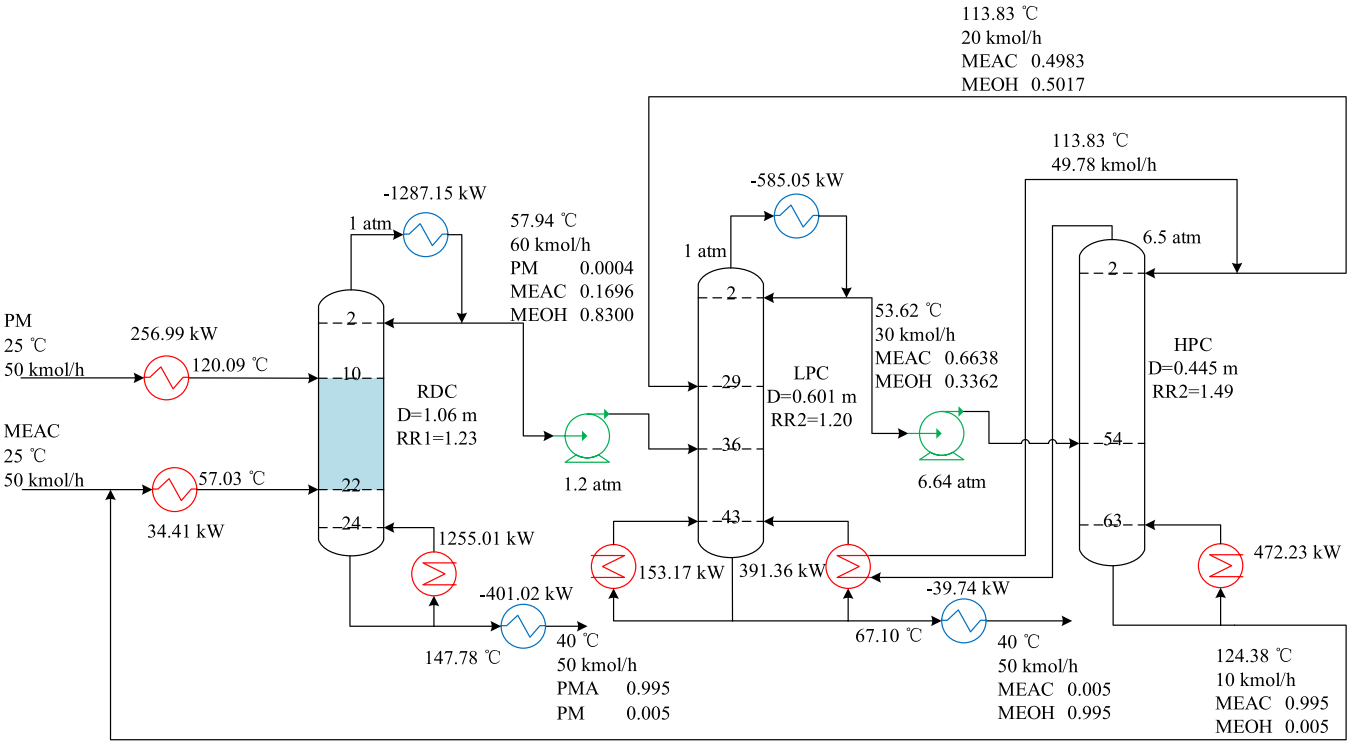

Figure 6. Flow sheet of the PHI-RDPSD.

22 of RDC. The RDC distillate is the MEAC/MEOH mixture and then is fed on stage 36 of LPC. 50 kmol/h of 99.5% mole purity PMA is obtained from the RDC bottom. The next column is the LPC which is operated at 1 atm with a 0.0027 pressure drop. The total stage number of the LPC is 44. The MEAC/MEOH mixture which contains 66.7% mole purity MEAC and 33.3% mole purity MEOH is taken from the LPC distillate with a flow rate of 30 kmol/h. Then the distillate stream is fed on stage 54 of HPC. 99.5% mole purity MEOH is withdrawn from the LPC bottom. The last column is the HPC which is operated at 6.5 atm with a 0.0027 pressure drop. The MEAC/MEOH mixture with a flow rate of 20 kmol/h and a composition of

DOI: 10.1021/acs.iecr.9b04122
Ind. Eng. Chem. Res. 2019, 58, 19211−19225

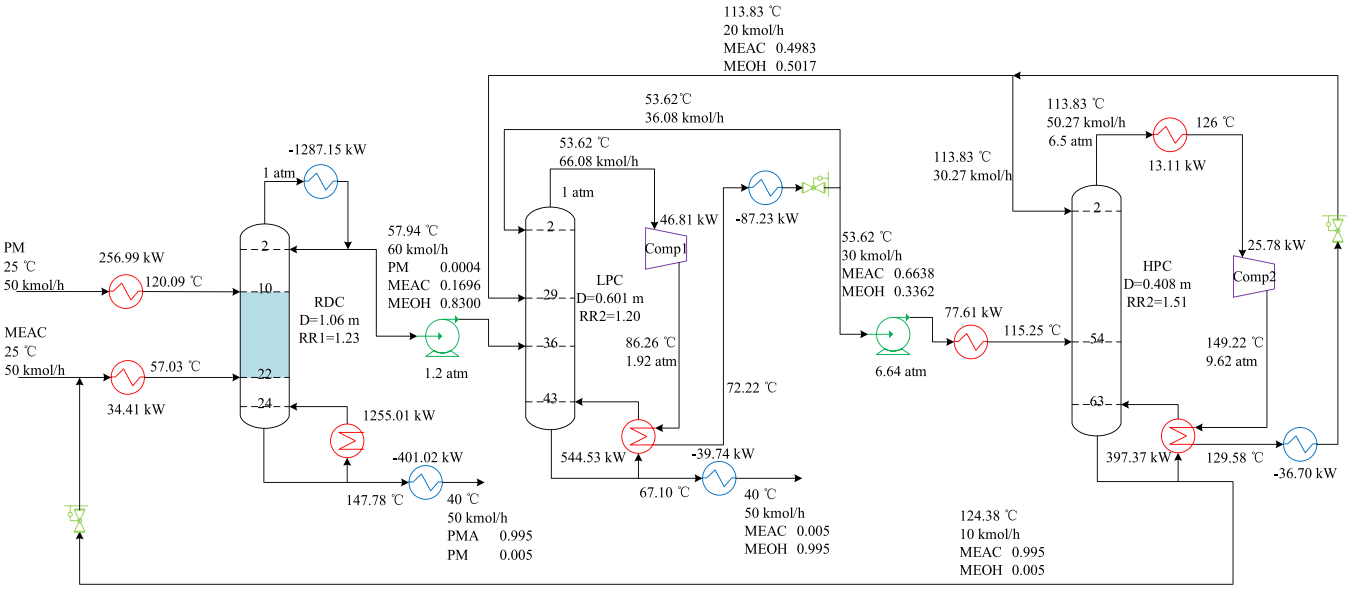

Figure 7. Flow sheet of the RDPSDVR-L-L.

49.83% mole purity MEAC and 50.17% mole purity MEOH is withdrawn from the HPC distillate. The HPC distillate is produced as the recycle stream to recycle back to stage 29 of LPC. The bottom stream of HPC is the 99.5% mole purity MEAC, which is mixed with fresh feed MEAC and is recycled to the stage 22 of RDC with a 10 kmol/h flow rate. The TAC calculated for the RDPSD is 11.42×10^5 $. Compared with the two-column RD, 24.35% of TAC is decreased in RDPSD. After the MEAC-MEOH azeotrope is separated by the PSD, the pure MEAC is fed back into the RDC in the RDPSD. To ensure the transesterification reaction of the RDC proceeds, the flow rate of the recycle stream in the two-column RD is more than that in the RDPSD, so that the energy requirements of RDPSD are less than that of the two-column RD. The OC of RDPSD decreases by 25.72% compared with two-column RD. Furthermore, with the flow rate of the recycle stream decreasing, the diameter of the column decreases. Though there are three columns in the RDPSD, the CI of the RDPSD decreases by 12.18% compared with that of the two-column RD. As a result, the RDPSD which shows better economic performance can be an alternative to the two-column RD for PMA synthesis.

3.3. Partial Heat-Integrated RDPSD Process. In the RDPSD process, because of the large temperature difference between the condenser of the HPC and the reboiler of the LPC, the heat integration can be introduced into the PSD. As a result, the energy consumption of PSD is able to be further saved. The heat duty of the condenser in the HPC is 391.36 kW, and the heat duty of the reboiler in the LPC is 544.53 kW. The heat duty of the condenser and the reboiler are different so that an auxiliary reboiler can be considered. As shown in Figure 6, an optimized partial heat-integrated RD and PSD combined process is designed in the study, which is called PHI-RDPSD. In the HPC, the top stream can provide heat to bottom reboiler of LPC. The other flow sheet of the PHI-RDPSD is the same with that of the RDPSD. The TAC calculated for the PHI-RDPSD is 9.888×10^5 $. Because a part of heat in the reboiler of LPC is provided by the condenser of HPC, the steam consumption is reduced effectively. As a result, 34.52% of TAC is reduced in PHI-RDPSD compared with the TAC of the two-column RD.

3.4. The RDPSD with Vapor Recompression. The reboilers in the RDPSD require much high-grade heat, meanwhile, the low-grade heat in the condensers is wasted. Thus, the vapor recompression which is able to change the low-grade heat to high-grade heat is introduced into the RDPSD process. The reboilers of RDPSD are heated by the distillate streams in RDC, LPC, and HPC. There are two choices for the vapor stream which is utilized to provide heat to the reboiler of the LPC. The one is the top vapor stream of LPC, which is called the L-L process. Another is the vapor stream in RDC, which is called the R-L process.

3.4.1. The RDPSD with Vapor Recompression for the L-L Process. The energy consumption of RDPSD can be saved through the introduction of the vapor recompression, and the reboiler of each column is heated by the distillate streams of LPC and HPC. A RDPSD with vapor recompression for the L-L process is designed in the study, which is named the RDPSDVR-L-L. The flowsheet of the RDPSDVR-L-L is illustrated in Figure 7. The LPC distillate is compressed in a compressor to reach an elevated thermal level. The work of the compressor is adjusted to ensure that the temperature of compressed stream is 5 K more than that of the stream in the reboiler. Then the heat resource in the reboiler of LPC is provided by the top compressed stream through the heat exchanger. After that, the distillate stream is condensed to 53.62 °C and then is split into two flows; one flow is recycled back to the top stage of LPC with a flow rate of 36.08 kmol/h, and the other is fed to the preheater with a flow rate of 30 kmol/h. The LPC bottom is 99.5% mole purity MEOH. After being heated to the bubble point temperature by the preheater, the outlet stream of the preheater is fed on stage 54 of HPC. After being preheated to 126 °C, the HPC distillate is compressed for a higher thermal level via the compressor. After providing heat to the reboiler in HPC, the compressed distillate stream is decreased to 113.83 °C by cooling water. The condensed stream is then split into two flows; one is refluxed to the HPC with a flow rate of 30.27 kmol/h, and the other is fed on stage 29 of LPC with a flow rate of 20 kmol/h. The bottom stream of HPC is the 99.5% mole purity MEAC which is mixed with fresh feed MEAC and is recycled to the stage 22 of RDC with a flow rate of 10 kmol/h. The other flowsheet in

DOI: 10.1021/acs.iecr.9b04122
Ind. Eng. Chem. Res. 2019, 58, 19211−19225

RDPSDVR-L-L is the same as that of the RDPSD. The TAC calculated for the RDPSDVR-L-L is 8.765 × 10^5 $, which is decreased by 41.96% compared with the TAC of the two-column RD.

3.4.2. The RDPSDVR-L-L Combined with Heat Exchanger Network. The temperature-heat (T-H) diagram of the RDPSDVR-L-L is illustrated in Figure 8. The heating and cooling requirements in the RDPSDVR-L-L account for 1637.13 kW and 1851.84 kW, respectively. The HEN is applied into the RDPSDVR-L-L to balance the hot and cold loads effectively, which can result in the reduction of energy consumption of the RDPSDVR-L-L. The process combined with the HEN is named as the RDPSDVR-L-L-HEN. Figure 9 illustrates the HEN which is implemented in Aspen Energy Analyzer for the RDPSDVR-L-L. The final HEN consists of a preheater (PreH), seven heat exchangers (E-n), four condensers (C-n), a reboiler (Reb), and two compressors (Comp-n). The RDC distillate is completely condensed by C1 (1287.15 kW), and the duty of Reb is 1255.01 kW. The heat in the bottom product stream of RDC is transferred to the HPC distillate by E6 (13.11 kW), the feed PM by E1 (256.99 kW), and the feed stream of HPC by E4 (21.96 kW), respectively. Then the product stream is condensed to 40 °C by C3 (108.96 kW). The temperature of the LPC distillate increases from 53.62 to 109.05 °C via Comp1 (46.81 kW). The compressed stream exchanges heat with the reboiler of LPC by E3 (544.53 kW). After that, the compressed stream preheats the feed MEAC to 57.03 °C by E2 (34.41 kW) and then is condensed to 53.62 °C in the C2 (52.82 kW). The bottom product steam of LPC is condensed to 40 °C by C4 (39.74 kW). After being heated by the E4 and E5 (36.70 kW), the feed stream of HPC is further heated to 115.25 °C through the PreH (18.95 kW). The HPC distillate at 113.83 °C is heated to 126 °C through E6 (13.11 kW). The heated stream increases to 149.22 °C via Comp2 (25.78 kW). After the compressed stream exchanges heat with the reboiler of HPC by E7 (397.37 kW), the compressed stream is cooled by E5 and leaves at 113.83 °C.

Figure 10 illustrates the T-H diagram for RDPSDVR-L-L-HEN. The heating requirement of RDPSDVR-L-L-HEN decreases from 1637.13 kW to 1273.96 kW (approximately 22.18%), while the cooling requirements of RDPSDVR-L-L-

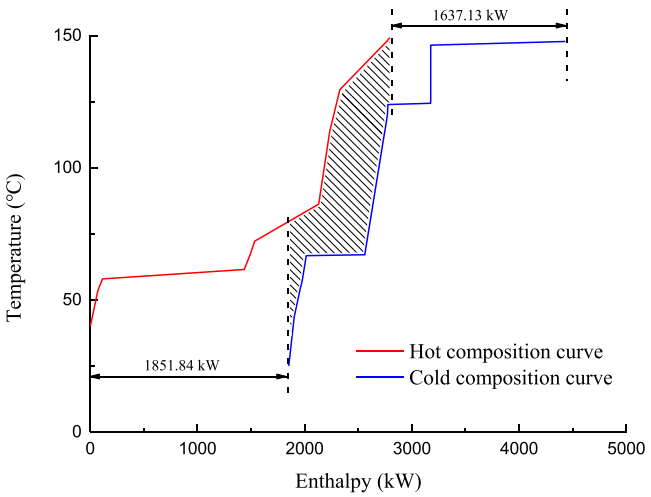

Figure 8. T-H diagram of the RDPSDVR-L-L.

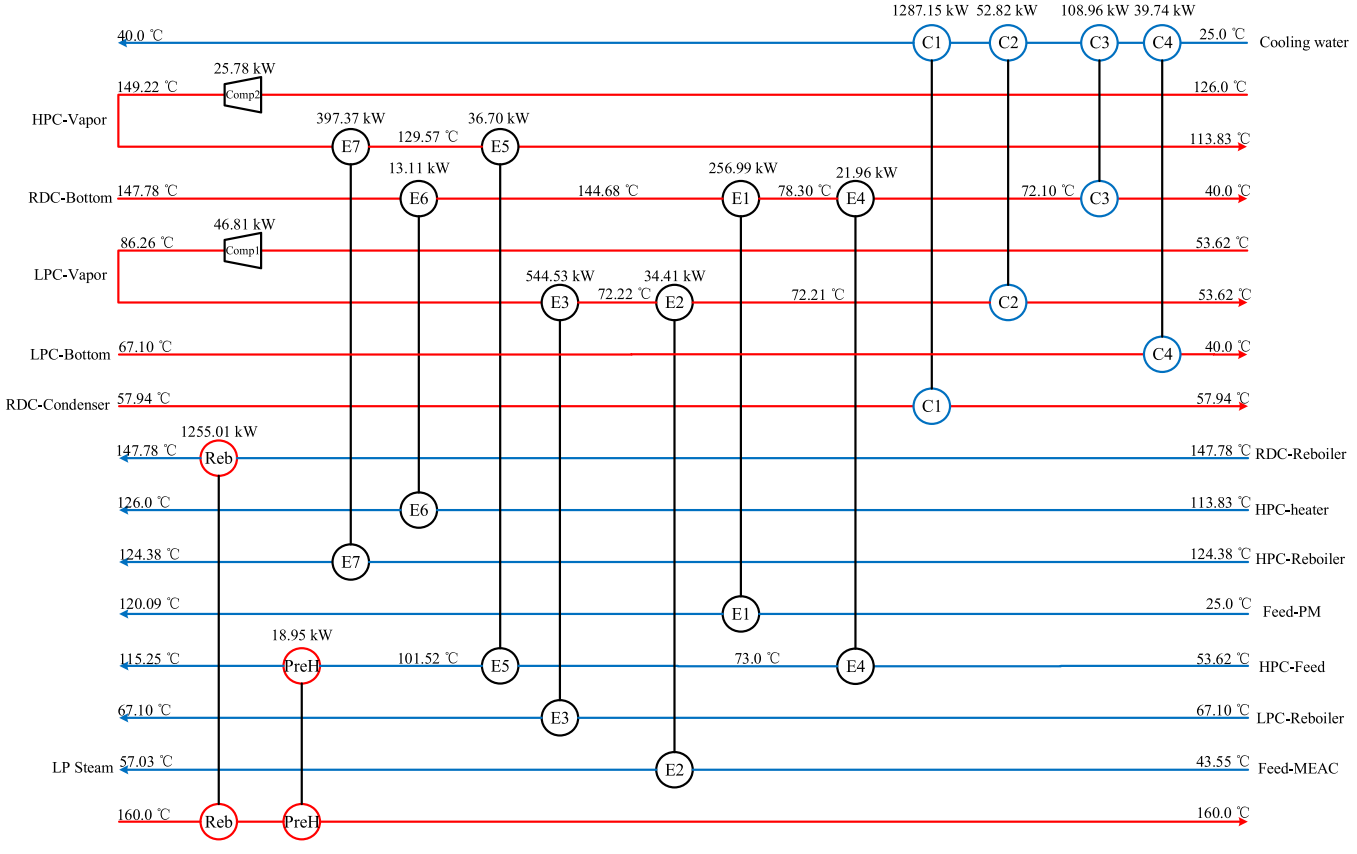

Figure 9. HEN of the RDPSDVR-L-L-HEN.

DOI: 10.1021/acs.iecr.9b04122
Ind. Eng. Chem. Res. 2019, 58, 19211−19225

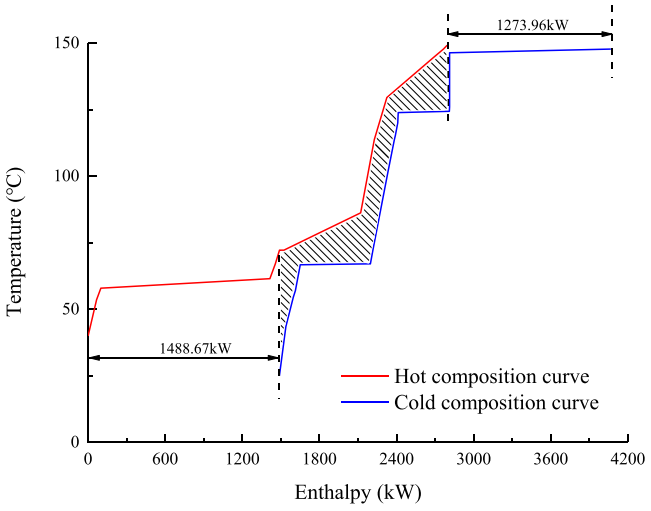

Figure 10. T-H diagram of the RDPSDVR-L-L-HEN.

HEN decrease from 1851.84 kW to 1488.67 kW (approximately 19.61%) compared with that of RDPSDVR-L-L. The minimum temperature difference is set as 5 K, and the pinch temperature is 72.7 °C.

Figure 11 shows the flow sheet of RDPSDVR-L-L-HEN. The TAC calculated for the RDPSDVR-L-L-HEN is 7.370×10^5 \$. Due to the introduction of HEN, more sensible heat is recovered in RDPSDVR-L-L-HEN. Therefore, 51.20% of TAC is reduced in the RDPSDVR-L-L-HEN compared with the TAC of two-column RD. Meanwhile, the TAC of RDPSDVR-L-L-HEN decreases by about 15.92% more than that of the RDPSDVR-L-L.

3.4.3. The RDPSD with Vapor Recompression for the R-L Process. Due to the temperature of the condenser in RDC being similar to that of the reboiler in LPC, thus, the latent heat of the condenser in RDC can also be utilized to boil up the liquid flow in the reboiler of LPC. A RDPSD with vapor recompression for the R-L process is designed in the study, which is named as the RDPSDVR-R-L. The flowsheet of the RDPSDVR-R-L is shown in Figure 12. The RDC distillate is separated into two flows. After being cooled to 57.94 °C, the one stream is refluxed to the RDC with a flow rate of 73.72 kmol/h. The other is compressed for the higher temperature and pressure through the compressor. The temperature of compressed stream should be 5 K more than that of the stream in the reboiler by changing the compressor work. Then the heat resource in the reboiler of LPC can be provided by the compressed stream through the heat exchanger. The stream coming from the heat exchanger is fed on stage 36 of LPC. After being pumped to 6.64 atm by the pump and heated to the bubble point temperature at 6.64 atm by the preheater, the distillation stream of LPC is fed on stage 54 of HPC. The other flow sheet of the RDPSDVR-R-L is the same as that of the RDPSDVR-L-L. The TAC calculated for the RDPSDVR-R-L is 8.663×10^5 \$, which decreases by 42.64% compared with the TAC of the two-column RD. Furthermore, compared with the RDPSDVR-L-L, 1.17% of the TAC is saved in the RDPSDVR-R-L.

3.4.4. The RDPSDVR-R-L Combined with the Heat Exchanger Network. Figure 13 presents the T-H diagram for RDPSDVR-R-L. The heating requirement and cooling requirement of the process account for 1637.13 kW and 1839.41 kW, respectively. The application of HEN is able to balance the hot and cold loads in RDPSDVR-L-L effectively, so that it can result in the reduction of energy consumption of the RDPSDVR-L-L. The process combined with the HEN is named as the RDPSDVR-R-L-HEN . Figure 14 illustrates the HEN of RDPSDVR-R-L which is implemented in Aspen Energy Analyze. The final HEN contains a preheater (PreH), seven heat exchangers (E-n), five condensers (C-n), a reboiler (Reb), and two compressors (Comp-n). The RDC distillate is

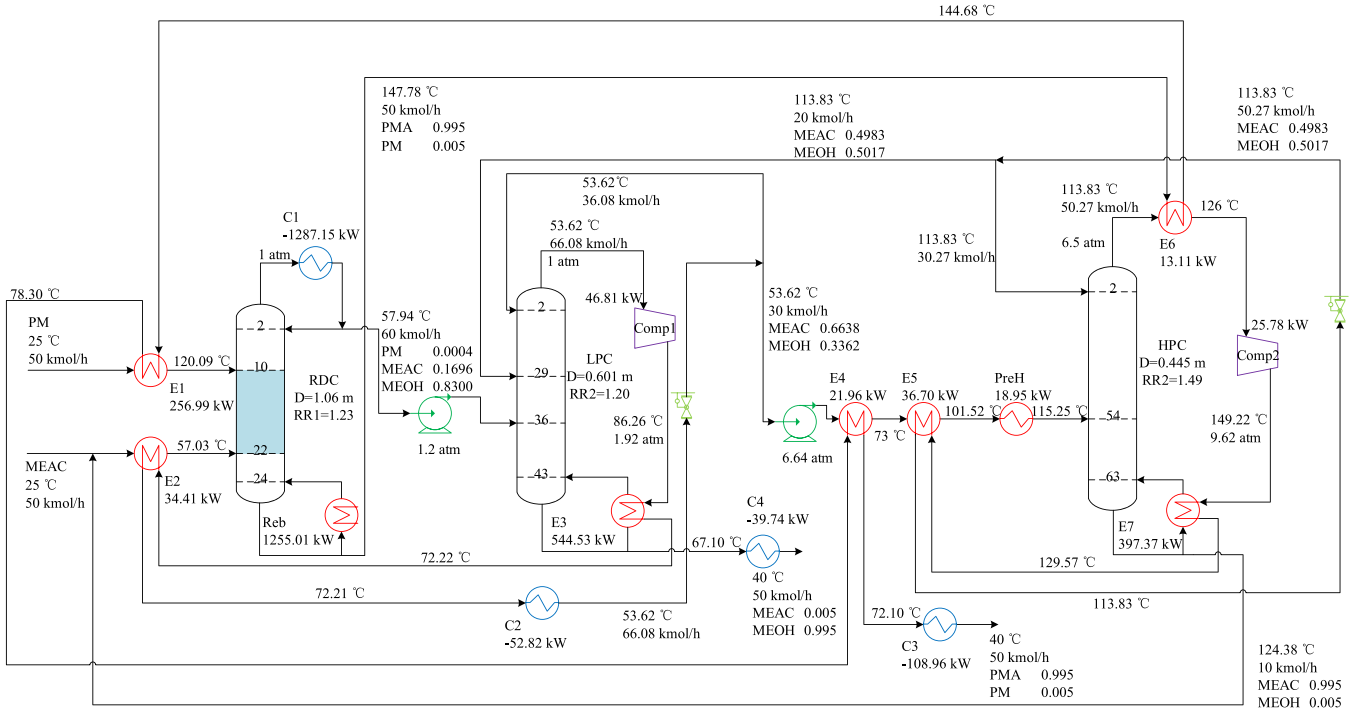

Figure 11. Flow sheet of the RDPSDVR-L-L-HEN.

DOI: 10.1021/acs.iecr.9b04122
Ind. Eng. Chem. Res. 2019, 58, 19211−19225

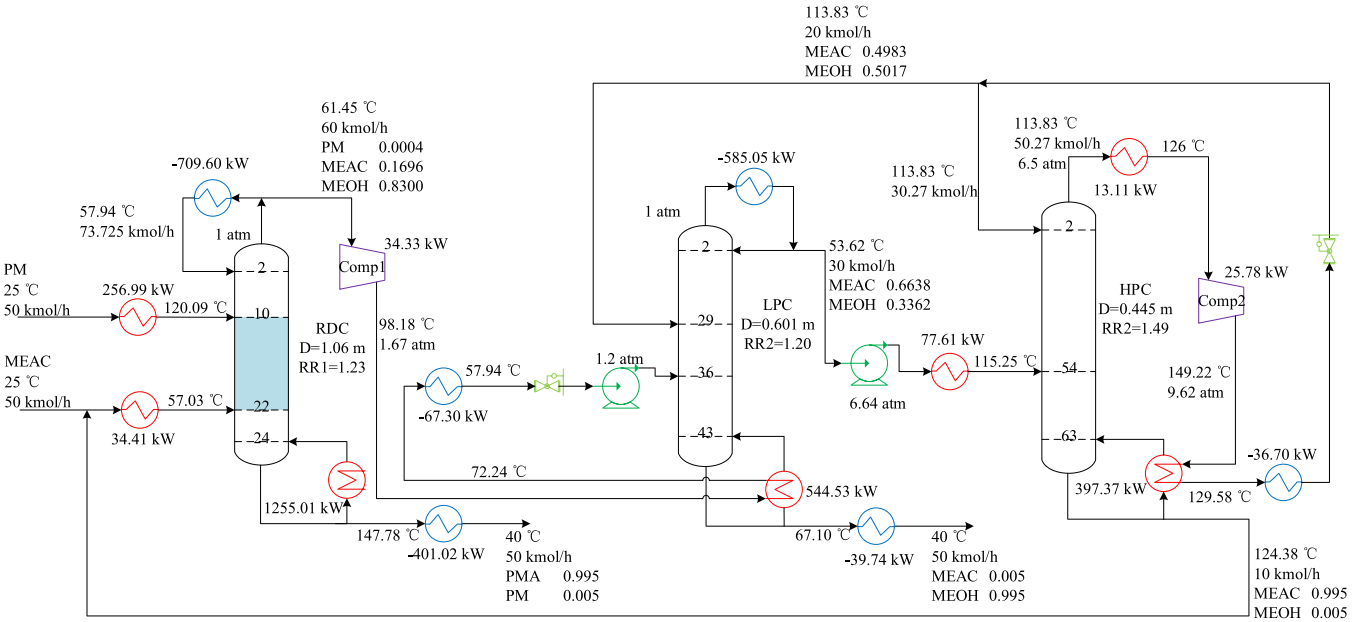

Figure 12. Flow sheet of the RDPSDVR-R-L.

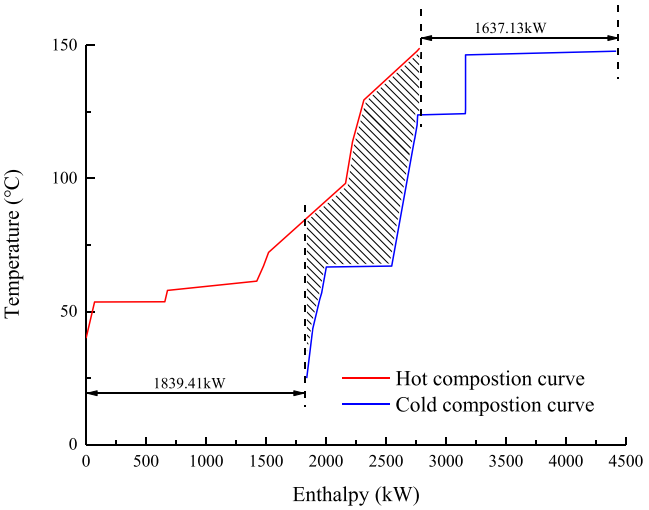

Figure 13. T-H diagram of the RDPSDVR-R-L.

separated into two flows. After being cooled to 57.94 °C by C1 (709.60 kW), the one flow is refluxed to the RDC. The temperature of the other flow is increased to 98.18 °C in the Comp1 (34.33 kW). The compressed stream exchanges heat with the bottom reboiler in the LPC by the E3 (544.53 kW). After that, the compressed stream preheats the feed MEAC to 57.03 °C by E2 (34.41 kW) and then is cooled to 57.94 °C in C2 (32.89 kW). The duty of Reb in RDC is 1255.01 kW. The heat in the RDC product stream is transferred to the HPC distillate by E6 (13.11 kW), the feed PM is transferred by E1 (256.99 kW), and the feed stream of HPC is transferred by E4 (21.96 kW), respectively. Then the product stream is cooled to 40 °C in C4 (108.96 kW). The LPC distillate is cooled to 53.62 °C by C3 (585.05 kW). After being heated by the E4 and E5 (21.96 kW), the distillation stream of the LPC is further preheated to 115.25 °C through PreH (18.95 kW) and then is fed into the HPC. The bottom product steam of LPC is condensed to 40 °C by C5 (39.74 kW). The HPC distillate is heated from 113.83 to 126 °C by the E6. After being compressed to 149.22 °C by Comp2 (25.78 kW), the top stream transfers heat to the bottom reboiler in HPC via the E7 (397.37 kW). Then the vapor stream is cooled to 113.83 °C by E5.

The T-H diagram for RDPSDVR-R-L-HEN is shown in Figure 15. The heating requirements of RDPSDVR-R-L-HEN decrease from 1637.13 kW to 1273.96 kW (approximately 22.18%), meanwhile, the cooling requirements in RDPSDVR-R-L-HEN are reduced from 1839.41 kW to 1476.24 kW (approximately 19.74%) compared with that of the RDPSDVR-R-L.

Figure 16 presents the flow diagram for the RDPSDVR-R-L-HEN. The TAC calculated for the RDPSDVR-R-L-HEN is 7.274×10^5 $. Due to the introduction of HEN, sensible heat is further saved in RDPSDVR-L-L-HEN. Thus, compared with the TAC of two-column RD, the TAC of RDPSDVR-R-L-HEN decreases by 51.83%, which also decreases by about 16.03% more than that of the RDPSDVR-R-L.

4. RESULTS COMPARISON AND ANALYSIS

4.1. Economic Evaluation. The TAC of proposed processes is listed in Table 4. The TAC of the RDPSD is 24.35% less than that of the two-column RD. In the RDPSD, the MEOH-MEAC azeotrope is separated through the PSD process, and the pure MEAC is fed back into the RDC with a low flow rate. As a result, more energy consumption can be saved in the RDC. The OC of RDPSD is 25.72% less than that of two-column RD. Furthermore, though the RDPSD has three columns, the diameters of the columns are smaller than that in two-column RD, so that the CI of RDPSD is 12.18% less than that of two-column RD.

Compared with the TAC of two-column RD, the PHI-RDPSD can achieve a 34.52% TAC saving. After the introduction of the heat integration, a part of heat in the reboiler of the LPC in the PHI-RDPSD can be provided from the condenser of HPC. Thus, the OC and CI of the PHI-RDPSD decrease by 37.05% and 12.12%, respectively.

Compared with the two-column RD, 41.96% and 42.64% of TAC are saved in the RDPSDVR-L-L and the RDPSDVR-R-L, respectively. After the introduction of vapor compression, the

DOI: 10.1021/acs.iecr.9b04122
Ind. Eng. Chem. Res. 2019, 58, 19211−19225

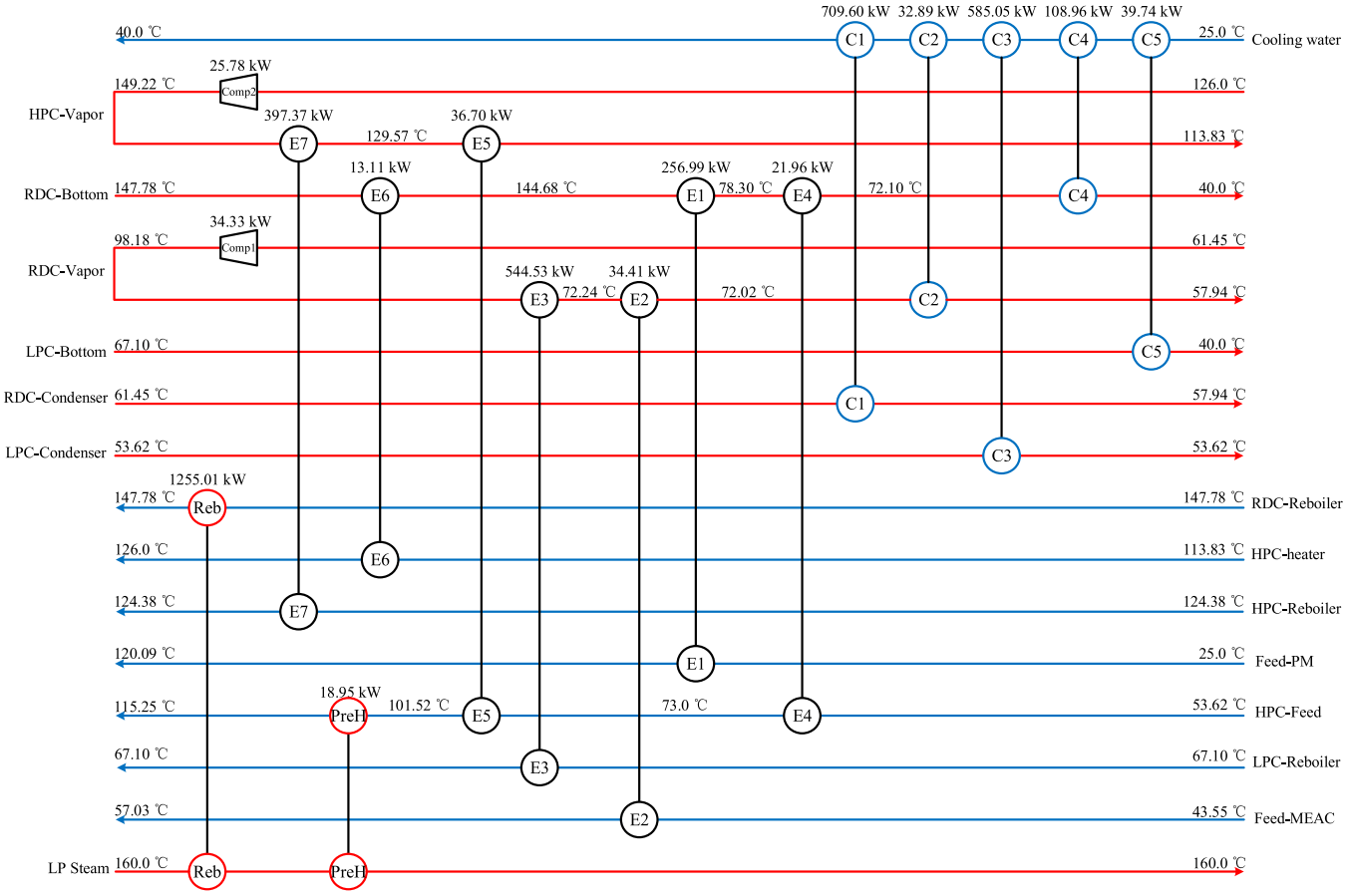

Figure 14. HEN of the RDPSDVR-R-L-HEN.

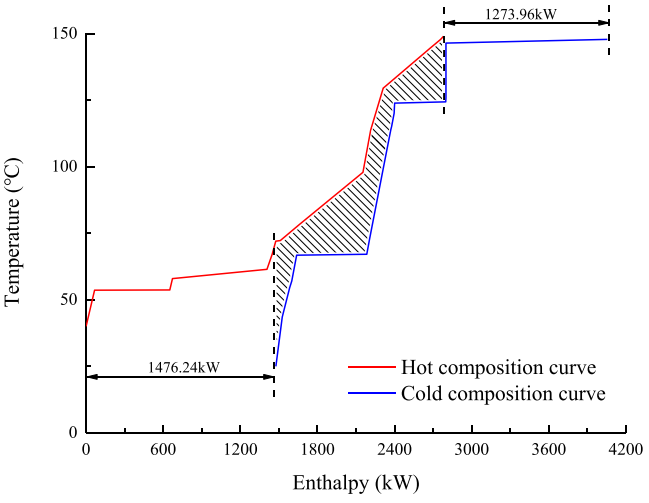

Figure 15. T-H diagram of the RDPSDVR-R-L-HEN.

bottom liquid streams in the LPC and the HPC are boiled up through the compressed streams. Compared with the two-column RD, 48.15% and 48.90% of the OC are decreased in the RDPSDVR-L-L and RDPSDVR-R-L. Because of the addition of the compressors, the CI of the RDPSDVR-L-L and RDPSDVR-R-L increases by 12.91% and 12.86% compared with that of two-column RD, respectively. Therefore, the TAC of RDPSDVR-L-L and RDPSDVR-R-L which combined with the OC and the CI is reduced compared with the two-column RD.

The HEN helps the RDPSDVR-L-L-HEN and RDPSDVR-R-L-HEN save more sensible heat. Compared with the two-column RD, the OC of the RDPSDVR-L-L-HEN and RDPSDVR-R-L-HEN decreases by 58.66% and 59.41%, respectively. However, because of the addition of heat exchangers, the CI of RDPSDVR-L-L-HEN and RDPSDVR-R-L-HEN increases by 14.93% and 15.31% compared with that of the two-column RD, respectively. As a result, 51.20% and 51.83% of TAC are saved in the RDPSDVR-L-L-HEN and RDPSDVR-R-L-HEN compared with that of two-column RD.

The vapor recompression system shows better performance with low temperature difference across the vapor recompression system. The temperature difference across the vapor recompression system in the RDPSDVR-R-L is smaller than that in the RDPSDVR-L-L. Compared with the RDPSDVR-L-L, the compression ratio of the Comp1 in the RDPSDVR-R-L is decreased, resulting in the reduction of the cost of equipment and electricity. The CI and OC of the RDPSDVR-R-L have a 0.04% and 1.45% reduction compared with that of RDPSDVR-L-L, respectively. Therefore, compared with the RDPSDVR-L-L, 1.17% of the TAC is saved in the RDPSDVR-R-L. As shown in Figure 17, the RDPSDVR-L-R-HEN shows the best economic performance.

4.2. Total Energy Requirements Evaluation. The total energy requirements (TER) have been calculated for the evaluation of proposed processes in energy-saving performance. The TER is calculated according to the equation[30]

$$\mathrm{TER} = Q_{\mathrm{R}} + Q_{\mathrm{Pre}} + f \cdot Q_{\mathrm{comp}} \quad (2)$$

DOI: 10.1021/acs.iecr.9b04122
Ind. Eng. Chem. Res. 2019, 58, 19211−19225

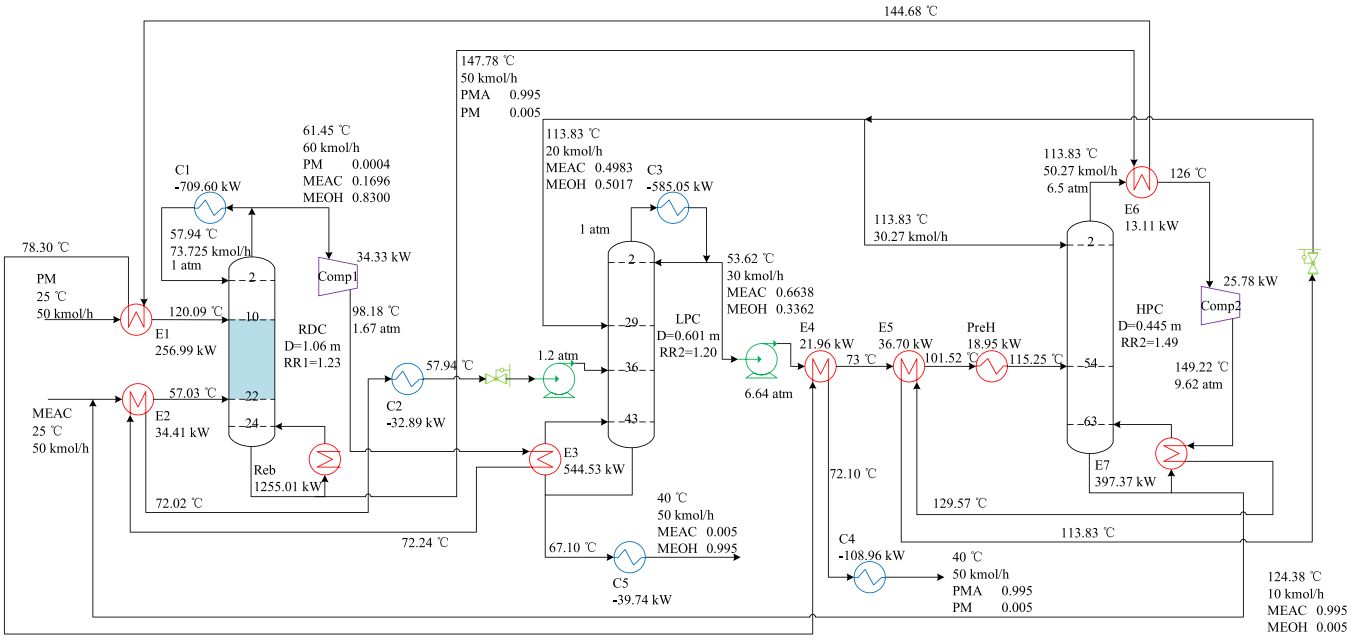

Figure 16. Flow sheet of the RDPSDVR-R-L-HEN.

Table 4. Economic Comparisons of the Seven Processes

	two-column RD	RDPSD	PHI-RDPSD	RDPSDVR-L-L	RDPSDVR-L-L-HEN	RDPSDVR-R-L	RDPSDVR-L-R-HEN
column vessel costs/10^5 $	5.274	4.992	4.992	4.848	4.848	4.849	4.849
heat exchangers costs/10^5 $	6.982	5.772	5.778	6.782	7.031	7.083	7.383
compressor costs/10^5 $				2.207	2.207	1.900	1.900
annual steam cost/10^5 $	13.20	9.803	8.306	6.261	4.872	6.261	4.872
annual cooling water cost/10^5 $	0.366	0.276	0.236	0.189	0.152	0.188	0.151
electricity costs//10^5 $				0.585	0.585	0.485	0.485
capital investment/10^5 $	12.26	10.76	10.77	13.84	14.09	13.83	14.13
annual operation cost/10^5 $	13.57	10.08	8.542	7.036	5.609	6.934	5.508
8 years TAC/10^5 $	15.10	11.42	9.888	8.765	7.370	8.663	7.274
TAC saving		24.35%	34.52%	41.96%	51.20%	42.64%	51.83%

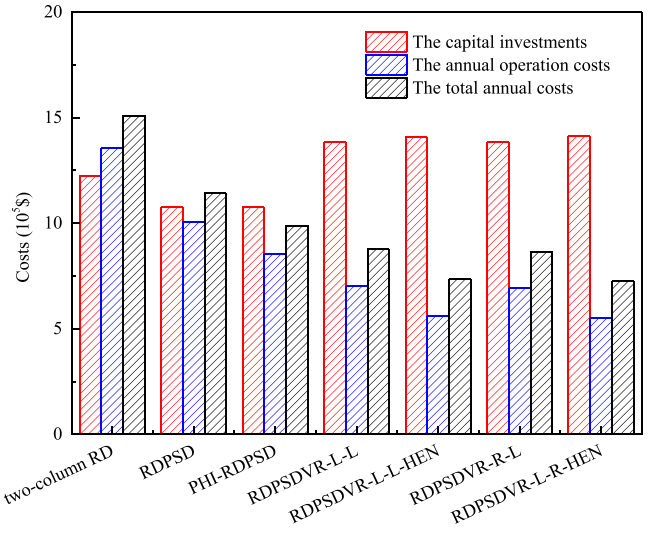

Figure 17. Comparison of required costs of the seven processes.

where Q_R (kW) presents the duty of reboilers, Q_{Pre} (kW) denotes the duty of preheaters, and Q_{comp} (kW) presents the work of the compressors. It should be mentioned that f which is the multiplication factor used to make Q_{comp} has the same effect of thermal power with the compressor electricity; the value of f is equal to 3 in this study.[31]

The TER for proposed processes is shown in Figure 18. Compared with the two-column RD, the TER of the RDPSD decreases by 25.75%. The PSD process can separate the MEAC-MEOH homogeneous azeotrope effectively in the RDPSD, so that the high purity MEAC with a low flow rate is fed back into the RDC. As a result, the TER in RDPSD is decreased compared with that of two-column RD.

Compared with the two-column RD, the TER of PHI-RDPSD decreases by 37.09%. The reboiler of the LPC is heated partially by the HPC distillate through the heat integration in the PHI-RDPSD. Thus, a part of reboiler duty of LPC can be saved.

Compared with the two-column RD, 46.27% and 47.35% of TER are reduced in the RDPSDVR-L-L and the RDPSDVR-R-L, respectively. In the RDPSDVR-L-L and RDPSDVR-R-L, after being introduced into the vapor compression system, the heat resource of reboilers in LPC and HPC can be provided from the compressed streams, so that the reboiler duty of the two processes can be saved. Due to the addition of the compressors, the work of the compressors is increased, but the energy requirements of the compressors are much less than the reboilers of LPC and HPC in the processes. As a result, the TER of RDPSDVR-L-L and RDPSDVR-R-L has an effective

DOI: 10.1021/acs.iecr.9b04122
Ind. Eng. Chem. Res. 2019, 58, 19211−19225

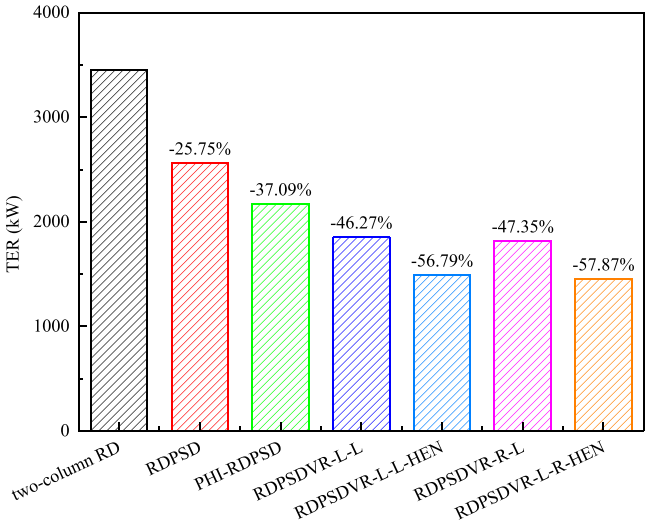

Figure 18. Comparison of TER of the seven processes.

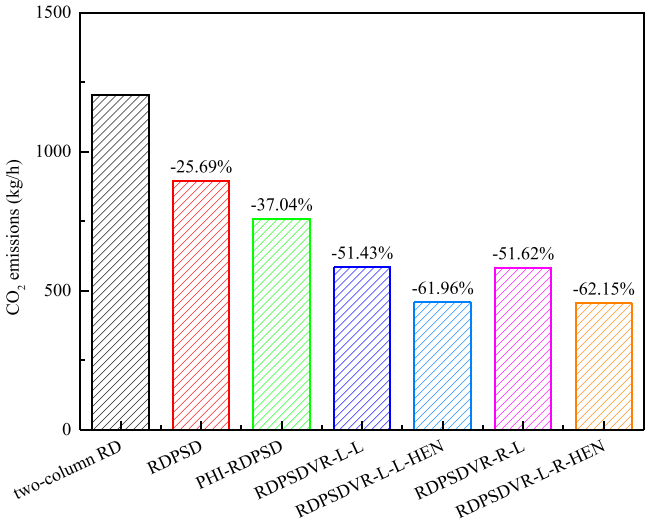

Figure 19. Comparison of CO_2 emissions of the seven processes.

reduction compared with that of two-column RD. Furthermore, the temperature difference of the vapor recompression system of RDPSDVR-R-L is smaller than that of RDPSDVR-L-L, so that the compression ratio of Comp1 of RDPSDVR-R-L is smaller than that of RDPSDVR-L-L. Thus, the compressors in the RDPSDVR-R-L require less energy compared with the RDPSDVR-L-L. As a result, compared with the RDPSDVR-L-L, 2.02% of TER is saved in the RDPSDVR-R-L.

In the RDPSDVR-L-L-HEN and RDPSDVR-R-L-HEN, the number of preheaters is decreased by using the HEN. Thus, the energy requirements of the preheaters are reduced. Compared with the TER of two-column RD, the TER of RDPSDVR-L-L-HEN and RDPSDVR-R-L-HEN decreases by 56.79% and 57.87%, respectively. Figure 18 shows that the RDPSDVR-R-L-HEN is the best process.

4.3. CO_2 Emissions Evaluation. The environmental performance of a process can be evaluated by calculating the CO_2 emissions. The calculation equation of CO_2 emissions (kg/s) is shown as follows[32]

$$[CO_2]_{emissions} = (Q_{Fuel}/NHV)(C\%/100)\alpha \quad (3)$$

where α, which presents the ratio of molar masses of CO_2 and C, is equal to 3.67. Q_{Fuel} (kW) presents the quantity of fuel required. In this study, heavy fuel oil is used to provide heat. NHV stands for the net heating value which is 39771 kJ/kg. While C%, which is carbon content, is equal to 86.5 in this study.

Q_{Fuel} is the heat duty provided by the steam according to the following calculation equation

$$Q_{Fuel} = \left(\frac{Q}{\lambda}\right)(h - 419)\left(\frac{T_{FTB} - T_0}{T_{FTB} - T_{stack}}\right) \quad (4)$$

where Q (kW) presents the total heat duty of process. λ (kJ/kg) and h (kJ/kg) are latent heat and enthalpy of steam in the process. T_{FTB} presents flame temperature with a value of 1800 °C, T_{Stack} is the stack temperature with a value of 160 °C, and T_0 denotes the ambient temperature.

The CO_2 emissions from the electricity power of compressors is set as 51.1 kg CO_2/GJ.[33]

Figure 19 illustrates the CO_2 emissions for proposed processes. CO_2 emissions of the RDPSD decrease by 25.69% compared with that of the two-column RD. In the RDPSD, the MEAC-MEOH azeotrope is separated by the PSD process, so that the flow rate of the pure MEAC stream which recycles back to the RDC is low. Thus, compared with the two-column RD, the recycle stream of RDPSD with lower flow rate further reduces the energy consumption of two-column RD, thus, the CO_2 emissions of the RDPSD are less than that of two-column RD.

Compared with the two-column RD, 37.04%, 51.43%, 61.96%, 51.62%, and 62.15% of CO_2 emissions are saved in the PHI-RDPSD, RDPSDVR-L-L, RDPSDVR-R-L, RDPSDVR-L-L-HEN, and RDPSDVR-R-L-HEN, respectively. After the heat integration is applied into the RDPSD, the reboiler of LPC can be heated partially by the HPC distillate stream. A part of steam requirements can be saved in the PHI-RDPSD, thus, the CO_2 emissions of PHI-RDPSD are reduced compared with the two-column RD. In the RDPSDVR-L-L and RDPSDVR-R-L, the reboilers of LPC and HPC can be heated through the top vapor streams by using the vapor compression system. The latent and sensible heat in the RDPSDVR-L-L and RDPSDVR-R-L are effective to be used, thus, the CO_2 emissions of the RDPSDVR-L-L and RDPSDVR-R-L can be reduced effectively. However, the work of Comp1 in the RDPSDVR-R-L is less than that RDPSDVR-L-L, so that 0.39% of CO_2 emissions is saved in the RDPSDVR-R-L compared with the RDPSDVR-L-L. More sensible heat is reduced in the RDPSDVR-L-L and RDPSDVR-R-L by the application of the HEN. Therefore, the CO_2 emissions of the two processes are further decreased. Similarly, CO_2 emissions of the RDPSDVR-L-L-HEN are 0.5% more than that of RDPSDVR-R-L-HEN. According to Figure 19, the environmental performance of RDPSDVR-R-L-HEN is the best.

5. CONCLUSION

In this study, a two-column RD process and an RDPSD process are proposed for the PMA synthesis by the transesterification reaction between PM and MEAC. After the MEAC-MEOH azeotrope is separated through the PSD process, the high mole purity MEAC with a low flow rate is recycled back into the RDC to participate in the transesterification reaction. Thus, RDPSD shows better energy-saving performance compared with two-column RD, and RDPSD can be an alternative to two-column RD. The introduction of the heat integration is a common way to improve the energy-saving performance of the PSD process,

DOI: 10.1021/acs.iecr.9b04122
Ind. Eng. Chem. Res. 2019, 58, 19211−19225

and the energy requirements of PHI-RDPSD are reduced compared with that of RDPSD. Then the vapor compression is applied to the RDPSD, and two processes with vapor compression are designed which are RDPSDVR-L-L and RDPSDVR-R-L. Because of the recovery of the latent and sensible heat, the vapor compression system leads to the energy savings in RDPSDVR-L-L and RDPSDVR-R-L. The HEN can help the RDPSDVR-L-L and RDPSDVR-R-L save more sensible heat. Therefore, the energy requirements of RDPSDVR-L-L-HEN and RDPSDVR-R-L-HEN are further decreased. From the result of comparison, the heat integration, the vapor compression, and the HEN technology are able to improve the performance of RDPSD in varying degrees. It is also clear that the process with vapor compression shows better energy-saving performance with a smaller temperature difference across the vapor compression system. As a result, the RDPSDVR-R-L-HEN shows the best performance compared with other processes in this study. Compared with the two-column RD, the RDPSDVR-R-L-HEN decreases by 51.83% of the TAC, 57.87% of the TER, and 62.15% of the CO_2 emissions, respectively.

AUTHOR INFORMATION

Corresponding Author

*Phone: +86 519 86330355. Fax: +86 519 86330355. E-mail: huagonglou508@126.com.

ORCID

Qing Ye: 0000-0003-3257-9216

Notes

The authors declare no competing financial interest.

ACKNOWLEDGMENTS

We are thankful for the assistance from the staff at the Jiangsu Key Laboratory of Advanced Catalytic Materials and Technology from the School of Petrochemical Engineering (Changzhou University).

REFERENCES

(1) Oh, J.; Sreedhar, B.; Donaldson, M. E.; Frank, T. C.; Schultz, A. K.; Bommarius, A. S.; Kawajiri, Y. Transesterification of propylene glycol methyl ether in chromatographic reactors using anion exchange resin as a catalyst. *J. Chromatography A* **2016**, *1466*, 84−95.

(2) Wang, X.; Wang, Q.; Ye, C.; Dong, X.; Qiu, T. Feasibility Study of Reactive Distillation for the Production of Propylene Glycol Monomethyl Ether Acetate through Transesterification. *Ind. Eng. Chem. Res.* **2017**, *56* (25), 7149−7159.

(3) Wang, S. J.; Wong, D. S. H.; Yu, S. W. Design and control of transesterification reactive distillation with thermal coupling. *Comput. Chem. Eng.* **2008**, *32* (12), 3030−3037.

(4) Qiu, T.; Zhang, P.; Yang, J.; Xiao, L.; Ye, C. Novel Procedure for Production of Isopropanol by Transesterification of Isopropyl Acetate with Reactive Distillation. *Ind. Eng. Chem. Res.* **2014**, *53* (36), 13881−13891.

(5) Jiménez, L.; Costa-López, J. The Production of Butyl Acetate and Methanol via Reactive and Extractive Distillation. II. Process Modeling, Dynamic Simulation, and Control Strategy. *Ind. Eng. Chem. Res.* **2002**, *41* (26), 6735−6744.

(6) Suo, X.; Ye, Q.; Li, R.; Feng, S.; Xia, H. Investigation about Energy Saving for Synthesis ofIsobutyl Acetate in the Reactive Dividing-Wall Column. *Ind. Eng. Chem. Res.* **2017**, *56* (19), 5607−5617.

(7) Shen, L.; Wang, L.; Wan, H.; Guan, G. Transesterificationof Methyl Acetate with n-Propanol: Reaction Kinetics and Simulation in Reactive Distillation Process. *Ind. Eng. Chem. Res.* **2014**, *53* (10), 3827−3833.

(8) Fan, Y.; Ye, Q.; Cen, H.; Chen, J.; Liu, T. Design and optimization of reactive distillation processes for synthesis of isopropanol based on self-heat recuperation technology. *Chem. Eng. Res. Des.* **2019**, *147*, 171−186.

(9) Fair, J. R. Conceptual design of distillation system. By M. F. Doherty and M. F. Malone. McGraw-Hill, New York, 2001, 568 pp., $85.31. *AIChE J.* **2003**, *49* (9), 2452−2452.

(10) Cui, Y.; Shi, X.; Guang, C.; Zhang, Z.; Wang, C.; Wang, C. Comparison of pressure-swing distillation and heterogeneous azeotropic distillation for recovering benzene and isopropanol from wastewater. *Process Saf. Environ. Prot.* **2019**, *122*, 1−12.

(11) Yang, A.; Shen, W.; Wei, S.; Dong, L.; Li, J.; Gerbaud, V. Design and Control of Pressure-Swing Distillation for Separating Ternary Systems with Three Binary Minimum Azeotropes. *AIChE J.* **2019**, *65* (4), 1281−1293.

(12) Abu-Eishah, S. I.; Luyben, W. L. Design and control of a two-column azeotropic distillation system. *Ind. Eng. Chem. Process Des. Dev.* **1985**, *24* (1), 132−140.

(13) Zhang, Q.; Liu, M.; Li, W.; Li, C.; Zeng, A. Heat-integrated triple-column pressure-swing distillation process with multi-recycle streams for the separation of ternary azeotropic mixture of acetonitrile/methanol/benzene. *Sep. Purif. Technol.* **2019**, *211*, 40−53.

(14) Luo, B.; Feng, H.; Sun, D.; Zhong, X. Control of fully heat-integrated pressure swing distillation for separating isobutyl alcohol and isobutyl acetate. *Chem. Eng. Process.* **2016**, *110*, 9−20.

(15) Haelssig, J. B.; Tremblay, A. Y.; Thibault, J. Technical and Economic Considerations for Various Recovery Schemes in Ethanol Production by Fermentation. *Ind. Eng. Chem. Res.* **2008**, *47* (16), 6185−6191.

(16) Ferre, J. A.; Castells, F.; Flores, J. Optimization of a distillation column with a direct vapor recompression heat pump. *Ind. Eng. Chem. Process Des. Dev.* **1985**, *24* (1), 128−132.

(17) Jana, A. K.; Mane, A. Heat pump assisted reactive distillation: Wide boiling mixture. *AIChE J.* **2011**, *57* (11), 3233−3237.

(18) Xia, H.; Ye, Q.; Feng, S.; Li, R.; Suo, X. A novel energy-saving pressure swing distillation process based on self-heat recuperation technology. *Energy* **2017**, *141*, 770−781.

(19) Zhang, Q.; Liu, M.; Zeng, A. Performance enhancement of pressure-swing distillation process by the combined use of vapor recompression and thermal integration. *Comput. Chem. Eng.* **2019**, *120*, 30−45.

(20) Li, X.; Geng, X.; Cui, P.; Yang, J.; Zhu, Z.; Wang, Y.; Xu, D. Thermodynamic efficiency enhancement of pressure-swing distillation process via heat integration and heat pump technology. *Appl. Therm. Eng.* **2019**, *154*, 519−529.

(21) Linnhoff, B.; Hindmarsh, E. The pinch design method for heat exchanger networks. *Chem. Eng. Sci.* **1983**, *38* (5), 745−763.

(22) Yang, M.; Feng, X.; Liu, G. Heat integration of heat pump assisted distillation into the overall process. *Appl. Energy* **2016**, *162*, 1−10.

(23) Chen, J.; Ye, Q.; Liu, T.; Xia, H.; Feng, S. Improving the performance of heterogeneous azeotropic distillation via self-heat recuperation technology. *Chem. Eng. Res. Des.* **2019**, *141*, 516−528.

(24) Patraşcu, I.; Bîldea, C. S.; Kiss, A. A. Eco-efficient Downstream Processing of Biobutanol by Enhanced Process Intensification and Integration. *ACS Sustainable Chem. Eng.* **2018**, *6* (4), 5452−5461.

(25) Ye, C.; Dong, X.; Zhu, W.; Cai, D.; Qiu, T. Isobaric vapor−liquid equilibria of the binary mixtures propylene glycol methyl ether +propylene glycol methyl ether acetate, methyl acetate+propylene glycol methyl ether and methanol+propylene glycol methyl ether acetate at 101.3 kPa. *Fluid Phase Equilib.* **2014**, *367*, 45−50.

(26) Turton, R.; Bailie, R. C.; Whiting, W. B.; Shaeiwitz, J. A. *Analysis, synthesis and design of chemical processes*, 3rd ed.; Prentice Hall: 2011.

(27) Luyben, W. L. *Principles and Case Studies of Simultaneous Design*; Wiley & Sons: 2011; DOI: 10.1002/9781118001653.

(28) Luyben, W. L. Heat Exchanger Simulations Involving Phase Changes. *Comput. Chem. Eng.* **2014**, *67* (11), 133−136.

(29) Luyben, W. L. Series versus Parallel Reboilers in Distillation Columns. *Chem. Eng. Res. Des.* **2018**, *133*, 294−302.

DOI: 10.1021/acs.iecr.9b04122
Ind. Eng. Chem. Res. 2019, 58, 19211−19225

(30) Kumar, V.; Kiran, B.; Jana, A. K.; Samanta, A. N. A novel multistage vapor recompression reactive distillation system with intermediate reboilers. *AIChE J.* **2013**, *59* (3), 761−771.
(31) Iwakabe, K.; Nakaiwa, M.; Huang, K.; Nakanishi, T.; Røsjorde, A.; Ohmori, T.; Endo, A.; Yamamoto, T. Energy saving in multi-component separation using an internally heat-integrated distillation column (HIDiC). *Appl. Therm. Eng.* **2006**, *26* (13), 1362−1368.
(32) Gadalla, M. A.; Olujic, Z.; Jansens, P. J.; Jobson, M.; Smith, R. Reducing CO_2Emissions and Energy Consumption of Heat-Integrated Distillation Systems. *Environ. Sci. Technol.* **2005**, *39* (17), 6860−6870.
(33) Yang, A.; Sun, S.; Eslamimanesh, A.; Shen, W. Energy-saving investigation for diethyl carbonate synthesis through the reactive dividing wall column combining the vapor recompression heat pump or different pressure thermally coupled technique. *Energy* **2019**, *172*, 320−332.

DOI: 10.1021/acs.iecr.9b04122
Ind. Eng. Chem. Res. 2019, 58, 19211−19225